ELSEVIER

15 June 1998

OPTICS COMMUNICATIONS

Optics Communications 152 (1998) 161–167

Full length article

Normalized optimization of second harmonic effects in slab waveguides

O. Parriaux [a,*], G.J. Veldhuis [b], H.J.W.M. Hoekstra [b], D. Blanc [a]

[a] *Laboratoire TSI, Université Jean-Monnet, 23, rue du Dr. P. Michelon, F-42023 Saint-Etienne, France*
[b] *Twente University, MESA Institute, PO Box 217, 7500 AE Enschede, The Netherlands*

Received 5 January 1998; revised 16 February 1998; accepted 9 March 1998

Abstract

A method for the optimization of $\chi^{(2)}$ coupling phenomena in slab waveguides on the basis of reduced parameters is presented. It is shown that the configuration for maximum second harmonic generation (SHG) efficiency is given by a single chart with two normalized parameters only. This optimization procedure is illustrated for the case of SHG in the nonlinear cladding of a linear step index waveguide. © 1998 Elsevier Science B.V. All rights reserved.

Keywords: Harmonic generation; Nonlinear waveguide; Optical polymers and organics; Optical waveguide and couplers

1. Introduction

The overlap of the fundamental and second harmonic fields in a nonlinear medium and the phase mismatching between them are two important physical parameters governing the efficiency of second harmonic generation (SHG). In a free space wave configuration a large field overlap is naturally obtained when the coupled waves are co-propagating, whereas phase matching is achieved by properly adjusting the orientation of the nonlinear material, a crystal usually, with respect to the polarization of the fundamental and of the second harmonic waves. A number of pulsed as well as CW frequency-doubled lasers are now available on the market [1]. A further degree of freedom in the optimization of the coupling coefficient between the two waves is now possible in free space wave devices by achieving a periodical poling all through the volume of the nonlinear crystal [2]. This allows the use of the highest nonlinear susceptibility component while maintaining the synchronism between the coupled waves by a periodical 'quasi-phase-matching' (QPM) scheme [3].

Great efforts are now devoted in research and industrial laboratories [4,5] to smaller size and lower pump power green and blue lasers. The obvious solution is to perform the nonlinear interaction in a waveguide configuration. This results in a large magnification of the interacting fields for the same propagated power over a nonlimited interaction length. However, there is a price for this: on one hand it is more difficult to fulfil the phase matching condition than it is in the bulk case, which imposes a QPM scheme which must be compatible with the waveguide technology. On the other hand, the field overlap in the nonlinear medium can only be made large by carefully selecting the symmetry of the interacting fields and by suitably adjusting the opto-geometrical parameters of the waveguide structure. At present this is made on a case-by-case basis, every new set of material and waveguide parameters imposing a re-optimization of the linear structure.

The present paper proposes a general optimization methodology for a three-layer system whereby all possible SHG waveguide structures of the slab and step index type can be optimally designed on the basis of two reduced optical parameters only. The basis of the formalism used here was first developed to give the general optimal design

* E-mail: parriaux@univ-st-etienne.fr

0030-4018/98/$19.00 © 1998 Elsevier Science B.V. All rights reserved.
PII S0030-4018(98)00150-3

of evanescent wave bio-chemical sensors of maximum sensitivity [6]. It is adapted here for the design of the waveguide structures achieving the maximum coupling coefficient between a fundamental wave and its second harmonics.

The optimization methodology is applied here in the particular case of a linear waveguide with a semi-infinite nonlinear cover made of a poled polymeric material. This is a practically interesting structure, for it alleviates the requirements of thickness accuracy and uniformity which are always very critical in the deposition of polymeric films. In such configuration, the nonlinear film thickness is not a critical parameter any more regarding the phase matching condition [7]. However, the fact that only the evanescent tail of the interacting fields 'sees' the nonlinear material limits the field overlap. It is consequently of prime importance to find the waveguide structure which maximizes it in the nonlinear overlay.

2. Methodology

The waveguide structure considered here is depicted in Fig. 1. It consists of a step index slab waveguide of thickness w, refractive index n_g, on a semi-infinite substrate of index n_s, coated with a semi-infinite cladding of index n_c. For simplicity zero material dispersion is assumed. This will lead to an incomplete description of the phase mismatch but to a reasonably accurate estimate of the coupling coefficients. In the algebraic developments which follow use will be made of the relative permittivity $\varepsilon_i = n_i^2$, i = s, g or c. n_e is the modal effective index [11] at frequency ω with $\varepsilon_e = n_e^2$. $\tilde{n}_e$ is the effective index of the coupled mode at frequency 2ω. λ is the wavelength at the fundamental frequency, $k_0 = 2\pi/\lambda$ is the corresponding vacuum wave number. The presented normalized formalism does not place any limitation on which waveguide modes get coupled, on the symmetry of the nonlinear material, and on which of the three layers is (are) nonlinear. However, for the sake of simplicity, a waveguide cladded with a nonlinear polymeric material with its poling performed normally to the waveguide interfaces will be considered as an example. In this case, the overlap integral in the coupling coefficient for SHG reduces to a particularly simple expression [8] where only TM–TM mode coupling leads to a significant coupling strength.

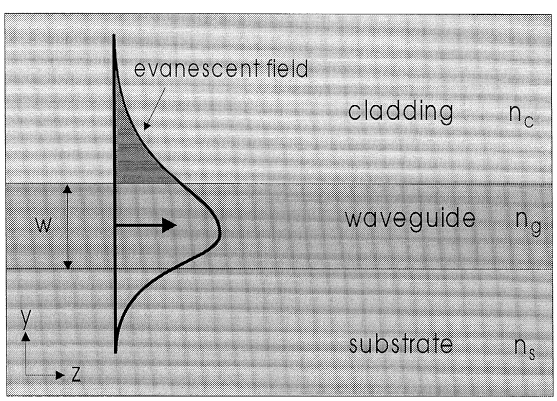


Fig. 1. Schematic representation of the discussed waveguide structure.

Assuming only one non-zero tensor component for SHG in the present case, $\chi^{(2)}_{yyy}$, written $\chi^{(2)}$ hereafter, and also that the modal effective indexes are not far from each other, the coupled mode equations between the TM_m mode at frequency ω and the TM_n mode at frequency 2ω as these propagate along z for real refractive indices (i.e. real fields) and real $\chi^{(2)}$ are [9]

$$\mathrm{i}\frac{\partial A_m}{\partial z} = \kappa A_m^* \tilde{A}_n \mathrm{e}^{\mathrm{i}\Delta\beta z}, \quad \mathrm{i}\frac{\partial \tilde{A}_n}{\partial z} = \kappa A_m^2 \mathrm{e}^{-\mathrm{i}\Delta\beta z}, \tag{1}$$

where the coupling coefficient κ is given by

$$\kappa = \frac{\omega\varepsilon_0}{2}\int \chi^{(2)} E_m^2 \tilde{E}_n \mathrm{d}y / P_{\mathrm{norm}}, \tag{2}$$

and $\Delta\beta = 2k_0(\tilde{n}_{en} - n_{em})$ is the phase mismatch term between the fundamental and SH modes.

Note that $\kappa \propto \sqrt{P_{\mathrm{norm}}}$.

$A_m(z)$ and $\tilde{A}_n(z)$ are the slowly varying amplitudes of the coupled modal fields of order m and n at the fundamental and SH frequencies respectively. $E_m(y)$ and $\tilde{E}_n(y)$ are the normalized modal field components of mode TM_m at frequency ω and of mode TM_n at frequency 2ω respectively, as given in Ref. [9]. $E_m(y)$ and $\tilde{E}_n(y)$ are both normal to the waveguide surface. Both normalized modes propagate the same power P_{norm} (e.g. 1 W/m) down the slab waveguide of thickness w and infinite width.

The case of quasi-phase matching (QPM) where the synchronism between the two coupled modes is restored by means of a perturbation of the nonlinear susceptibility $\chi^{(2)}$ [12] can be treated with the same coupled wave formalism. If K_g is the spatial frequency of the perturbation, the coupling coefficient in the case of first order grating coupling and of inverted domains of equal length, is given by

$$\kappa^{\mathrm{QPM}} = \kappa \times 2/\pi, \tag{3}$$

and the phase mismatch term is replaced by

$$\Delta\kappa^{\mathrm{QPM}} = 2k_0(\tilde{n}_{en} - n_{em}) \pm K_g, \tag{4}$$

depending on the sign of the used diffraction order of the grating.

Following the formalism developed in the case of evanescent wave sensors [6], the coupling coefficient κ

will now be expressed in terms of the normalized variables X_s and $\tilde{X}_s$, and normalized asymmetry parameters a_s and a_c defined hereafter: X_s and $\tilde{X}_s$ are the normalized effective index at ω and 2ω frequency respectively (all quantities with a tilde refer to the second harmonic)

$$X_s = \sqrt{\frac{\varepsilon_e - \varepsilon_s}{\varepsilon_g - \varepsilon_e}} \text{ and } X_c = \sqrt{\frac{\varepsilon_e - \varepsilon_c}{\varepsilon_g - \varepsilon_e}}$$

$$\text{with } X_c^2 = \frac{1 - a_c}{1 - a_s}\left(1 + X_s^2\right) - 1. \quad (5)$$

a_s and a_c are the asymmetry parameters $a_s = \varepsilon_s/\varepsilon_g$ and $a_c = \varepsilon_c/\varepsilon_g$. X_c is a practical auxiliary variable of X_s.

The condition for maximum coupling coefficient will be found analytically in the Appendix A to be the solution of a single transcendental equation of a single normalized variable X_s with only two normalized parameters a_s and a_c. This condition gives once and for all the optimum nonlinear configuration (i.e. thickness, w) for SHG in a step index waveguide with nonlinear cover whatever the refractive indexes n_s, n_g, n_c and λ. Once this maximum, i.e. $X_{smax}(a_s,a_c)$, is found, general results can advantageously and meaningfully be represented in the form a 3D chart showing the corresponding maximum coupling coefficient κ_{max} as a surface versus a_s and a_c using Eq. (A13). In order to keep all the generality of the obtained result, one does not represent κ as such but rather the normalized coupling coefficient $\bar{\kappa}$ which is given by $\bar{\kappa} = n_g\kappa/(\omega^{3/2}\chi^{(2)})$ in $(s^{3/2}\ V/m^2)$. Also it is important for the designer to know how the optimum structure: from

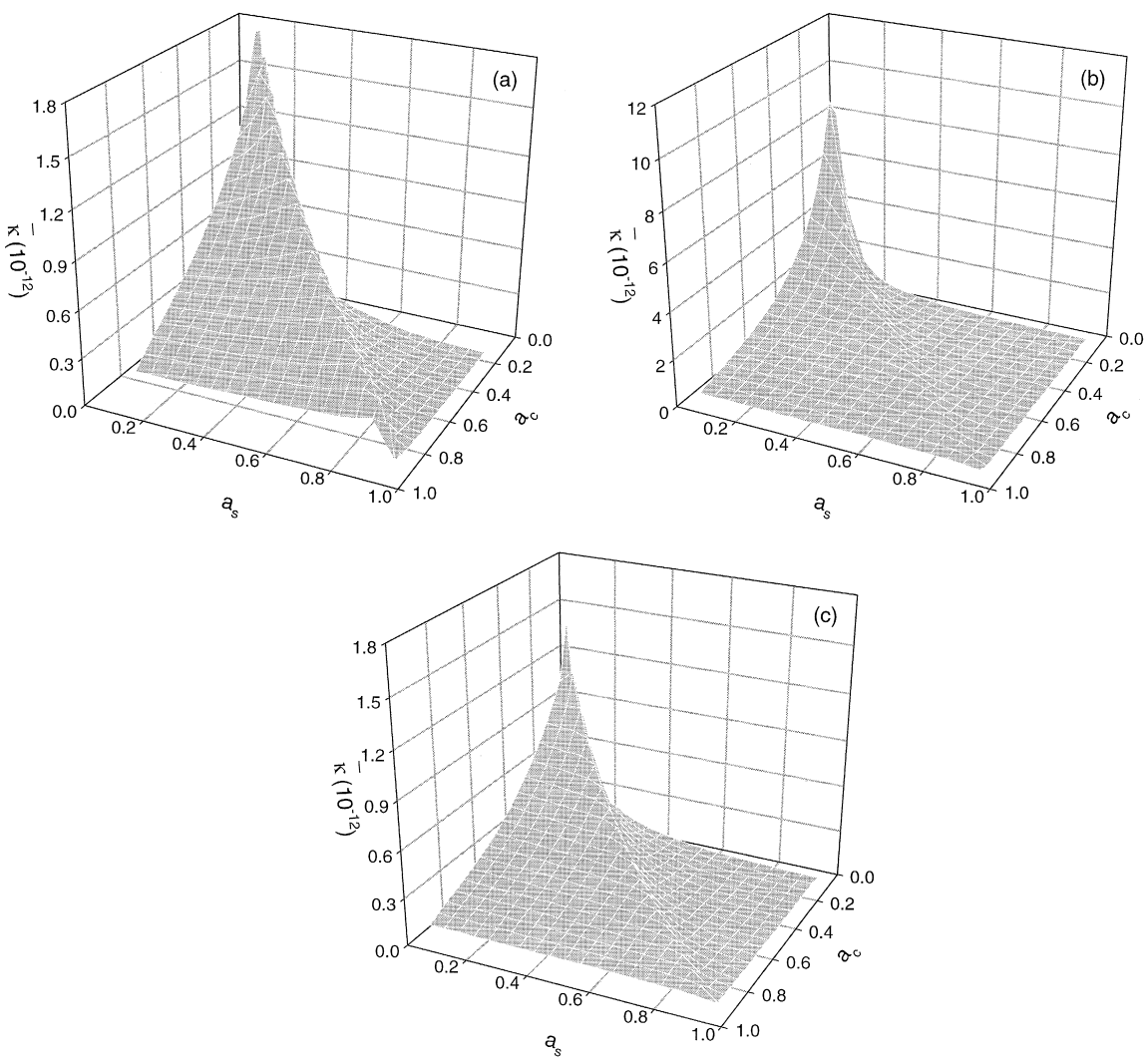


Fig. 2. Maximum achievable normalized coupling coefficient $\bar{\kappa}$ versus a_s and a_c for respectively (a) $TM_0(\omega)$–$TM_0(2\omega)$, (b) $TM_0(\omega)$–$TM_1(2\omega)$ and (c) $TM_0(\omega)$–$TM_2(2\omega)$ coupling.

the solution $X_{\mathrm{smax}}(a_s,a_c)$ one retrieves the value of $n_g w/\lambda$ ensuring a maximum coupling coefficient, $(n_g w/\lambda)_{\max}(a_s,a_c)$, given by Eq. (A16), which again can be represented as a surface in a 3D chart.

The optimum nonlinear structure is thus fully defined and the maximum expectable SHG efficiency is known. The designer is still interested in the phase mismatched under the condition of maximum coupling coefficient. Rather than representing $\Delta\beta$ versus a_s and a_c one prefers to represent the coherence length L_c defined as

$$L_c = \pi/\Delta\beta, \tag{6}$$

where $\Delta\beta$ was defined in Eq. (2). Here again, we will represent the coupling length in its most normalized form where the effective indices at ω and 2ω are expressed by means of X_s. Instead of L_c we represent $\bar{L}_c = L_c n_g/\lambda$ which writes:

$$\bar{L}_c = \frac{1}{4}\left[\sqrt{\frac{a_s + X_s^2}{1+X_s^2}} - \sqrt{\frac{a_s + \tilde{X}_s^2}{1+\tilde{X}_s^2}}\right]^{-1}. \tag{7}$$

This information will only tell which part of the total dispersion is due to the waveguide dispersion. It will not allow one to decide whether QPM is necessary and what the grating period must be. Having optimized the coupling condition for SHG, one has also de facto optimized for cascading effects which are proportional to the coupling coefficient [10].

3. Discussion of the normalized results

The algebraic results above can be used for any pair of TM modes at ω and 2ω frequencies. We will here only consider the dominant mode TM_0 at ω, and modes TM_0, TM_1 and TM_2 at frequency 2ω for reasons of practical interest.

Fig. 2a–2c represent the maximum coupling coefficient $\bar{\kappa}(a_s,a_c)$ which can be obtained in all three mode coupling cases. The figure reveals that the $TM_0(\omega)$–$TM_1(2\omega)$ coupling situation is more efficient than the other two situations by one order of magnitude. This is in contrast with the case where the waveguide itself is nonlinear where the zero crossing of the TM_1 mode inside the waveguide tends to cancel the overlap of the fields. For all three coupling situations we find that, the better the symmetry (a_s close to a_c), and the larger the guidance (a_s, a_c small), the larger $\bar{\kappa}$. Also $\bar{\kappa}$ is larger in the (a_s,a_c) plane section where $a_s < a_c$. From the definition of the ordinate $\bar{\kappa}$ of the charts, one can further state that the maximum coupling coefficient $\kappa_{\max}$ increases with a decrease of the waveguide index n_g, and with the power $2/3$ of the fundamental wavelength.

The charts of Fig. 3 show the normalized coherence length for $TM_0(\omega)$–$TM_1(2\omega)$ coupling and reveals that

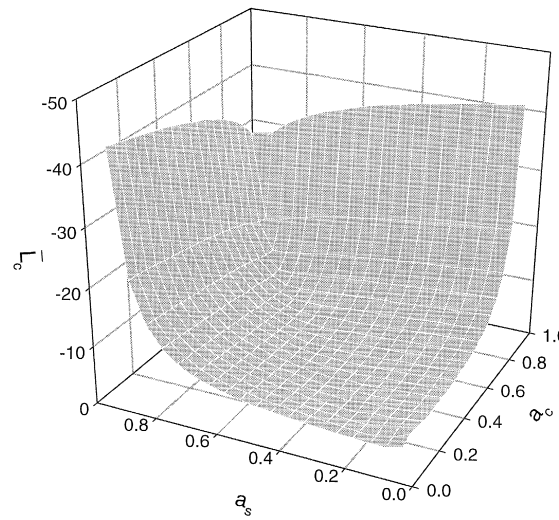


Fig. 3. Normalized coherence length, $\bar{L}_c$, corresponding to maximum $\bar{\kappa}$ versus a_s and a_c for $TM_0(\omega)$–$TM_1(2\omega)$ coupling.

the larger the asymmetry, the lower the guidance, the shorter the coherence length $\bar{L}_c$. The charts for the two other (less efficient) coupling cases, which are not presented here, show similar features. Remembering that large coherence length means good phase matching, one concludes that the conditions for large $\kappa_{\max}$ imply a large phase mismatch and conversely. The consequence for the design of an efficient SHG structure with nonlinear material in the cover only, which was expected to be tolerant on the deposition thickness, is that QPM is necessary as from the start unless strong anomalous material dispersion compensates for the phase mismatch due to waveguide dispersion.

Regarding the waveguide mode content as shown in Fig. 4a, 4b for the $TM_0(\omega)$–$TM_1(2\omega)$ case, where the meshed surfaces are the cut-off planes of the two lowest order modes, the study reveals that the waveguide at the fundamental frequency is single mode in all three cases. In the most favourable case, i.e. large $\bar{\kappa}$, the $TM_1(2\omega)$ mode is close to cut off [11].

In conclusion, it is shown that the conditions for a maximum SHG coupling coefficient in the case of a nonlinear cladding on a step index waveguide are fully determined by a single value of the sole normalized effective index which only depends on the dielectric symmetry of the structure via two normalized parameters. It was shown in particular that the only coupling situation of interest practically in the case of a nonlinear cover poled normally to the guide surface is that of $TM_0(\omega)$–$TM_1(2\omega)$. Finally, it was revealed that the condition of large coupling coefficient are also those for a large phase mismatch, thus imposing QPM.

This normalized formalism was applied here to the case of a nonlinear cover. It is readily applicable to more

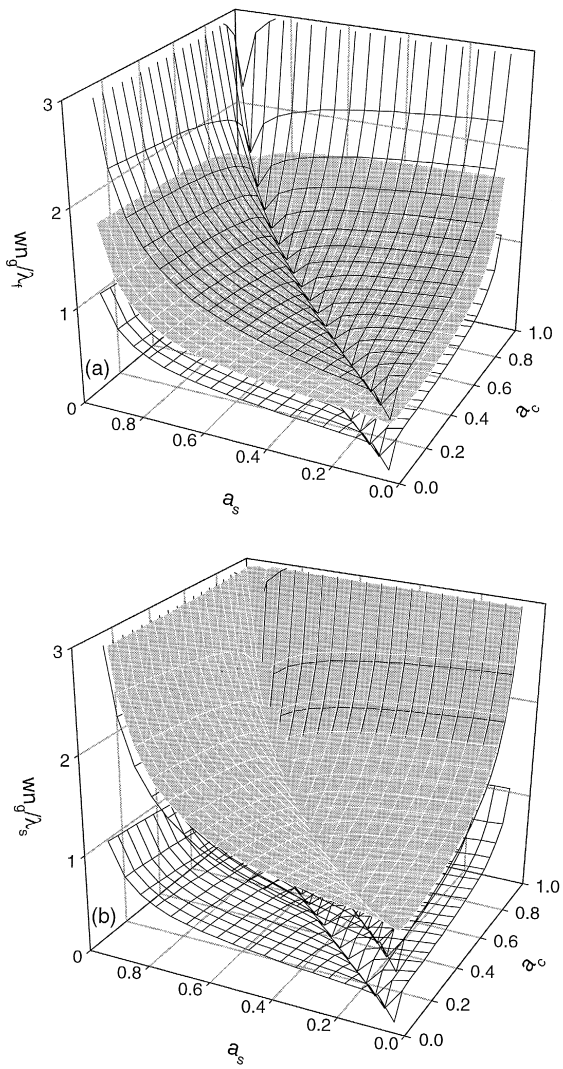


Fig. 4. Normalized optical thickness $n_g w/\lambda$ to corresponding to maximum $\bar{\kappa}$ versus a_s and a_c for $TM_0(\omega)$–$TM_1(2\omega)$ coupling for (a) the fundamental wavelength and (b) the second harmonic wavelength. The cut-off condition for the TM_0 and the TM_1 modes are indicated by the mesh.

efficient structures where two or three layers are nonlinear with possibly different $\chi^{(2)}$. This is likely to reveal interesting general features which will be reported later.

Acknowledgements

The authors are grateful to Dr. Kerstin Wörhoff, Dr. Gijs Krijnen and Professor Paul V. Lambeck, Lightwave Device Group at the MESA Institute of Twente University for their precious cooperation in the application of nonlinear optics and in checking the presented results. The authors thank Professor A. Cachard, Head of the TSI Laboratory for reading the manuscript. The work of G.J. Veldhuis was financially supported by the Dutch Innovative Research Program (IOP) Electro-Optics. Part of this work is supported by the EC, project INCO-Cop 96 194.

Appendix A. Derivation of the condition for maximum coupling coefficient

The coupling coefficient in the SHG process, κ, writes

$$\kappa = \frac{\omega}{2}\varepsilon_0 \int \chi^{(2)} E_y^2 \tilde{E}_y \,\mathrm{d}y / P_{\mathrm{norm}}, \tag{A1}$$

where E_y is the modal electric field component normal to the guide surface at the fundamental frequency and $\tilde{E}_y$ at the second harmonic (SH).

In a TM mode, the E_y field expression in the cover is [11]:

$$E_y = -\frac{\beta z_0^2}{\omega \mu_0 \varepsilon_c} A_c \exp\left[-k_0\sqrt{\varepsilon_e - \varepsilon_c}\,(y-w)\right], \tag{A2}$$

where w is the waveguide thickness, $z_0 = \sqrt{\mu_0/\varepsilon_0}$ is the impedance of vacuum, $\beta = n_e k_0$ is the propagation constant, and the amplitude A_c is a constant corresponding to P_{norm} [11]:

$$A_c^2 = \frac{4\varepsilon_g}{n_e z_0 \left(1 + \dfrac{\varepsilon_e - \varepsilon_c}{\varepsilon_g - \varepsilon_e}\dfrac{\varepsilon_g^2}{\varepsilon_c^2}\right) w_{\mathrm{eff}}} P_{\mathrm{norm}}. \tag{A3}$$

w_{eff} is the mode effective width which in the TM case is [11]:

$$w_{\mathrm{eff}} = w + \frac{1}{k_0\sqrt{\varepsilon_e - \varepsilon_c}\left\{\varepsilon_e\left(1/\varepsilon_c + 1/\varepsilon_g\right) - 1\right\}} + \frac{1}{k_0\sqrt{\varepsilon_e - \varepsilon_s}\left\{\varepsilon_e\left(1/\varepsilon_s + 1/\varepsilon_g\right) - 1\right\}} \tag{A4}$$

Eqs. (A2), (A3) and (A4) are valid at both fundamental and SH frequencies. As from now all quantities referring to the SH will be written with a tilde.

From this, and Eq. (5), we can establish some modular expressions which will be used frequently:

$$\frac{\varepsilon_e}{\varepsilon_g} = \frac{a_c + X_c^2}{1 + X_c^2} = \frac{a_s + X_s^2}{1 + X_s^2},$$

$$1 - \frac{\varepsilon_e}{\varepsilon_g} = \frac{1 - a_c}{1 + X_c^2} = \frac{1 - a_s}{1 + X_s^2},$$

$$\frac{\varepsilon_e}{\varepsilon_g} - a_c = X_c^2 \frac{1 - a_c}{1 + X_c^2}. \tag{A5}$$

Let us write Eqs. (A4), (A3) and (A2) with the normalized quantities:

$$w_{\mathrm{eff}} = \frac{1}{k_0 w\sqrt{\varepsilon_g}\,\sqrt{1-\varepsilon_e/\varepsilon_g}} \times \left\{ k_0 w\sqrt{\varepsilon_g}\,\sqrt{1-\varepsilon_e/\varepsilon_g} + \frac{1/X_c}{(\varepsilon_e/\varepsilon_g)(1/a_c+1)-1} + \frac{1/X_s}{(\varepsilon_e/\varepsilon_g)(1/a_s+1)-1} \right\}. \quad \text{(A6)}$$

Using Eq. (A5), and the fact that the term $k_0 w\sqrt{\varepsilon_g-\varepsilon_e}$ satisfies the characteristic equation for the mode TM_m, w_{eff} becomes [11]:

$$w_{\mathrm{eff}} = \frac{1}{n_g k_0}\sqrt{\frac{1+X_s^2}{1-a_s}}\;F, \quad \text{(A7)}$$

where

$$F = \tan^{-1}\frac{X_c}{a_c} + \tan^{-1}\frac{X_s}{a_s} + m\pi + \frac{a_c}{X_c}\frac{1+X_c^2}{a_c^2+X_c^2} + \frac{a_s}{X_s}\frac{1+X_s^2}{a_s^2+X_s^2}.$$

Eqs. (A2)–(A7) can be written similarly for the TM_n mode at the SH frequency, taking care that the frequency term is now 2ω:

$$\tilde{w}_{\mathrm{eff}} = \frac{1}{2n_g k_0}\sqrt{\frac{1+\tilde{X}_s^2}{1-a_s}}\;\tilde{F}, \quad \text{(A8)}$$

where

$$\tilde{F} = \tan^{-1}\frac{\tilde{X}_c}{a_c} + \tan^{-1}\frac{\tilde{X}_s}{a_s} + n\pi + \frac{a_c}{\tilde{X}_c}\frac{1+\tilde{X}_c^2}{a_c^2+\tilde{X}_c^2} + \frac{a_s}{\tilde{X}_s}\frac{1+\tilde{X}_s^2}{a_s^2+\tilde{X}_s^2}.$$

Expressed by means of the normalized variables and parameters (A5), the A_c^2 term of Eq. (A3) becomes:

$$A_c^2 = \frac{4\varepsilon_g P k_0}{z_0}\,a_c^2\sqrt{1-a_s}\;\frac{1}{\sqrt{a_s+X_s^2}\,(a_c^2+X_c^2)F}. \quad \text{(A9)}$$

At the SH frequency, similarly

$$\tilde{A}_c^2 = \frac{8\varepsilon_g P k_0}{z_0}\,a_c^2\sqrt{1-a_s}\;\frac{1}{\sqrt{a_s+\tilde{X}_s^2}\,(a_c^2+\tilde{X}_c^2)\tilde{F}}. \quad \text{(A10)}$$

The integral term I in the nonlinear cover is:

$$I = \int_w^\infty \exp\left[-2k_0(y-w)\left(\sqrt{\varepsilon_e-\varepsilon_c}+\sqrt{\tilde{\varepsilon}_e-\varepsilon_c}\right)\right]\mathrm{d}y, \quad \text{(A11)}$$

where the factor 2 accounts for the square of the fundamental frequency field and for the double frequency of the SH. Evaluation of Eq. (A11) leads to:

$$I = \frac{1}{2k_0 n_g\left(\sqrt{\varepsilon_e/\varepsilon_g-a_c}+\sqrt{\tilde{\varepsilon}_e/\varepsilon_g-a_c}\right)}. \quad \text{(A12)}$$

Regrouping all terms leads to an expression for κ which is the product of a constant term with a number of X_s dependent terms:

$$\kappa = \gamma A\left\{B\cdot F\cdot\left(\tilde{B}\cdot\tilde{F}\right)^{1/2}\right\}^{-1}, \quad \text{(A13)}$$

where

$$\gamma = \frac{2\sqrt{2}\,\mu_0\sqrt{\varepsilon_0}\,P_{\mathrm{norm}}^{1/2}\,\omega^{3/2}}{n_g}\,\frac{(1-a_s)^{3/4}}{(1-a_c)^{1/2}}\,\chi^{(2)},$$

$$A = \frac{\sqrt{a_s+X_s^2}\left(a_s+\tilde{X}_s^2\right)^{1/4}}{X_c/\sqrt{1+X_c^2}+\tilde{X}_c/\sqrt{1+\tilde{X}_c^2}},$$

$$B = \left(1+X_s^2\right)\left(a_c^2+X_c^2\right),$$

$$\tilde{B} = \left(1+\tilde{X}_s^2\right)\left(a_c^2+\tilde{X}_c^2\right).$$

Later on, the coupling coefficient will be represented graphically in its most normalized form, i.e., the ordinate will correspond to $\bar{\kappa} = (n_g/\omega^{3/2}\chi^{(2)})\kappa$ in $(\mathrm{s}^{3/2}\ \mathrm{V/m}^2)$.

The next step in the search for the maximum coupling coefficient is the observation that, for interaction between two selected modes, κ can be expressed as a function of only a_s, a_c and X_c. This follows from Eq. (5) and from the fact that the characteristic equation

$$k_0 w n_g = \frac{1}{\sqrt{1+X_s^2}}\left(\tan^{-1}\frac{X_s}{a_s}+\tan^{-1}\frac{X_c}{a_c}+m\pi\right) = \frac{1}{2\sqrt{1+\tilde{X}_s^2}}\left(\tan^{-1}\frac{\tilde{X}_s}{a_s}+\tan^{-1}\frac{\tilde{X}_c}{a_c}+n\pi\right) \quad \text{(A14)}$$

is satisfied at both fundamental and harmonic frequencies.

The condition for maximum coupling is

$$\frac{\partial\kappa}{\partial(n_g k_0 w)} = \frac{\partial\kappa}{\partial X_s}\frac{\partial X_s}{\partial(n_g k_0 w)} = 0. \quad \text{(A15)}$$

The second derivative term is always different from zero which implies

$$\frac{\partial\kappa}{\partial X_s} = 0. \quad \text{(A16)}$$

Eq. (A16) is a single variable (X_s) transcendental equation, which is solved by analytical differentiation followed

by numerical zero finding. Hereby using the fact that the variable X_c depends on X_s as expressed in Eq. (5), and that $\tilde{X}_s$ and $\tilde{X}_c$ are related to X_s through Eq. (A14).

References

[1] G. Randolph, Laser Focus World (April 1995) 121.
[2] A. Harada, Y. Nihei, Appl. Phys. Lett. 69 (1996) 2629.
[3] L.E. Myers, G.D. Miller, R.C. Eckardt, M.M. Fejer, R.L. Byer, W.R. Rosenberg, Optics Lett. 20 (1995) 52.
[4] K. Schneider, S. Schiller, J. Mlynek, Optics Lett. 21 (1996) 1999.
[5] F. Leplingard, P. Pierrard, J.P. Herriau, G. Bocqueho, SPIE 3099 (1997) 131.
[6] O. Parriaux, G.J. Veldhuis, J. Lightwave Technol., in press.
[7] K. Wörhoff, O.F.J. Noordman, H. Albers, P.V. Lambeck, N.F. van Hulst, Optics Comm. 124 (1996) 493.
[8] A.M. Bouchoux, D. Blanc, A. Trouillet, C. Plumereau, A. Cachard, Nonlinear Optics 16 (1997) 291.
[9] G.J.M. Krijnen, W. Torruellas, G.I. Stegeman, H.J.W.M. Hoekstra, P.V. Lambeck, IEEE J. Quantum Electron. 32 (1996) 729.
[10] G.I. Stegeman, D.H. Hagan, L. Torner, Opt. Quantum Electron. 28 (1996) 1691.
[11] O. Parriaux, in: O. Wolfbeis (Ed.), Fiber Optic Chemical Sensors and Biosensors, ch. 4, CRC, Boca Raton, FL, 1991, p. 111.
[12] G.A. Magel, M.M. Fejer, R.L. Byer, Appl. Phys. Lett. 56 (1990) 108.